# The collapse behaviour of plate girders subjected to shear and bending

# The Collapse Behaviour of Plate Girders Subjected to Shear and Bending

## Comportement à la ruine d'une poutre métallique à double té soumise à des efforts tranchants et de flexion

## Bruchverhalten von Blechträgern unter dem Einfluss von Querkräften und Biegemomenten

**H. R. EVANS** Senior Lecturer
**D. M. PORTER** Senior Lecturer
**K. C. ROCKEY** Professor and Head
Department of Civil and Structural Engineering,
University College, Cardiff, GB

**SUMMARY**

The paper presents a method for calculating the collapse load of a plate girder loaded in shear and bending and also presents details of a quick and accurate design method which is capable of predicting the failure loads of plate girders when loaded in shear, bending or by shear and bending.

**RÉSUMÉ**

L'article présente une méthode de calcul de la charge de rupture d'une poutre métallique à double té sous l'effet d'efforts tranchants et de flexion. Il présente aussi les détails d'une méthode de dimensionnement rapide et précise.

**ZUSAMMENFASSUNG**

Eine Methode für die Berechnung der Bruchlast von Blechträgern unter dem Einfluss von Querkräften und Biegemomenten sowie ein rasches und genaues Bemessungsverfahren werden vorgestellt.

## 1. INTRODUCTION

In recent papers, the authors [1,2,3] have presented a new method for predicting the ultimate load capacity of webplates loaded in shear. Since this method provides identical upper and lower bound solutions, it can be considered to provide an exact solution for the idealised girder considered. It has been established [2] that the method is capable of accurately predicting the failure load of test girders whose webplates are loaded in shear. Although allowance was made in the solution for the axial forces in the flanges produced by the action of the membrane field, the solution did not deal with the case where a significant bending moment acts with the shear force. This paper presents a method to determine the collapse load of plate girders subjected to combined shear and bending. The paper first considers the collapse behaviour of plate girders subjected to either shear or bending and then develops a method which is able to deal with the combined loading case. Finally the authors present a design method which is both quick and easy to use and is capable of accurately predicting the failure load of symmetrical and unsymmetrical girders reinforced by both transverse and longitudinal stiffeners.

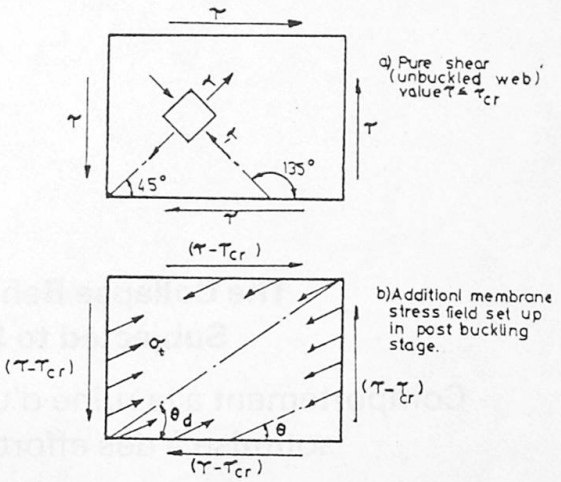


FIG. 1 - Stresses in a panel subjected to shear

## 2. WEBS LOADED IN SHEAR

An unbuckled shear web will develop equal tensile and compressive stresses inclined at 45° and 135° to the flanges, see Fig. 1(a). However, as shown by Wagner, when a webplate buckles, it is unable to carry any additional compressive loading and therefore has to develop a new load carrying mechanism in which the additional shear load is carried by an inclined tensile membrane field as shown in Fig. 1(b). Wagner determined expressions for the magnitude and inclination of this membrane field for the specific case where the webplate is very thin and the flanges are capable of carrying the lateral loading imposed by the membrane field without distorting enough to significantly influence the distribution of the membrane field. Although many studies were made to develop design methods [8,9] for the type of structures encountered in aeronautical engineering, these solutions were not suitable for the type of girders used in Civil Engineering, since these have flanges which will distort significantly and thereby influence the extent and nature of the membrane field which develops in the webplate.

The first ultimate load method which was capable of predicting the failure load of conventional plate girders was that proposed by Basler et al [4,5] in 1960. Basler assumed that the flanges of most plate girders were so flexible that they could not withstand the lateral loading imposed by an inclined tension field and established that in such cases the girder fails when the web panel develops an off-diagonal yield band BFEC, see Fig. 2, due to the presence of a tensile stress $\sigma_t^y$ which, acting together with those stresses occurring in the web at the instant of buckling, causes the web to 'yield' throughout its thickness. In addition, he assumed that the stresses in the adjacent triangular wedges ABC and EFD remained equal to those corresponding to the critical shear stresses $\tau_{cr}$.

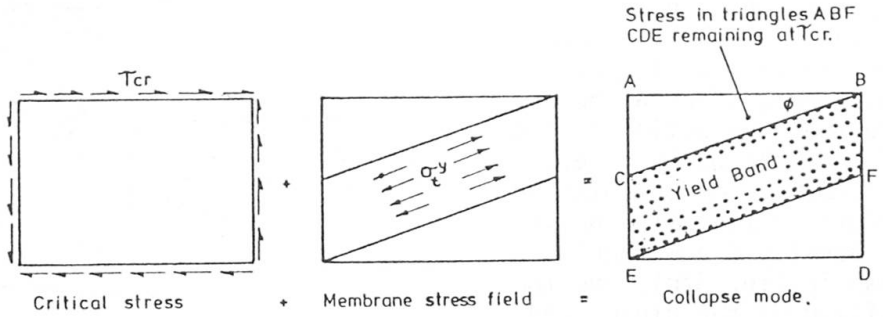


FIG. 2 - Ultimate load mechanism developed by Basler et al [4,5]

Clearly the assumption made by Basler that the flanges cannot withstand any lateral loading was very conservative. In 1968, Rockey and Skaloud [10,11] showed that for plate girders having proportions similar to those employed in Civil Engineering, the ultimate load capacity of plate girders was greatly influenced by the flexural rigidity of the flanges. They established that the collapse mode of plate girders involved the development of plastic hinges in the tension and compression flanges as shown in Fig. 3. Figures 4 and 5 show two experimental girders after they had been loaded to failure and it is clear that there is a close similarity between their mode of failure and that shown in Fig. 3. Since extensive strain gauge measurements indicated that the edge of the yield band intercepted the flanges very close to the position at which the plastic hinges formed, Rockey and Skaloud assumed that the width of the yield band was as indicated in Fig. 3, and that the membrane stress field was inclined in the direction of the panel diagonal.

In 1969, Fujii [12,13] presented a solution in which he considered the flanges to fail by the development of plastic hinges at their mid-panel positions together with hinges over the vertical stiffeners under the action of a uniformly distributed tension field.

Also in 1969, Chern and Ostapenko [14] presented a new version of the Basler collapse mechanism which allowed for a variation of the membrane stress across the webplate as shown in Fig. 6 and for the magnitude of $\sigma_t^y$ to vary with the inclination of the yield band. They used an optimisation process to find the value of $\theta$ which gives the maximum value of $V_{ult}$. In addition, Chern and Ostapenko stated that the flanges would contribute to the strength of the girder in assuming the development of a picture frame type of mechanism in which hinges form in the flanges over the transverse stiffeners.

In 1971, a solution by Komatsu [15] correctly postulated that girders would fail in the manner shown in Fig. 3 and recognised that the inclination of the tension membrane field would vary with the flange and panel properties. Unfortunately, however, this solution violates compatibility considerations in certain cases. In addition, when differentiating an expression to obtain that value of inclination $\theta$, which will maximise the ultimate load carrying capacity of the girder, it was incorrectly assumed that the position of the hinges was independent of the extent and inclination of the tension field.

The above theories were all discussed in detail at an International Colloquium [16] held in London in 1971. At this meeting, Ostapenko and Chern [17] and Rockey [18] presented papers in which their earlier solutions were extended to deal with the combined loading case of shear and bending, and also to provide solutions for the case of webplates reinforced by longitudinal stiffeners.

In 1973, Calladine [19] published an excellent paper in which he considered two specific cases. The first case was of a webplate with negligible buckling resistance, which allowed him to assume that the action of the web could be represented by a series of parallel tendons. He established that the girders would fail when the shear panels developed a mechanism of the form shown in Fig. 3(c), and that both the position of the hinges and the inclination of the membrane field varied with the rigidity of the flanges. The close similarity between the collapse model proposed by Calladine and the experimental evidence of Figs. 4 and 5 is very evident. Unfortunately, Calladine did not extend his solution to deal with practical girders where the web has a significant load carrying capacity before it buckles. The second case which Calladine considered was that of a very thick web which yields before it buckles and he showed that, in this case, failure would occur by the web yielding with the development of plastic hinges in the flanges at the corners of the web panel. It will be shown later that these solutions are two particular cases of the authors' present general solution.

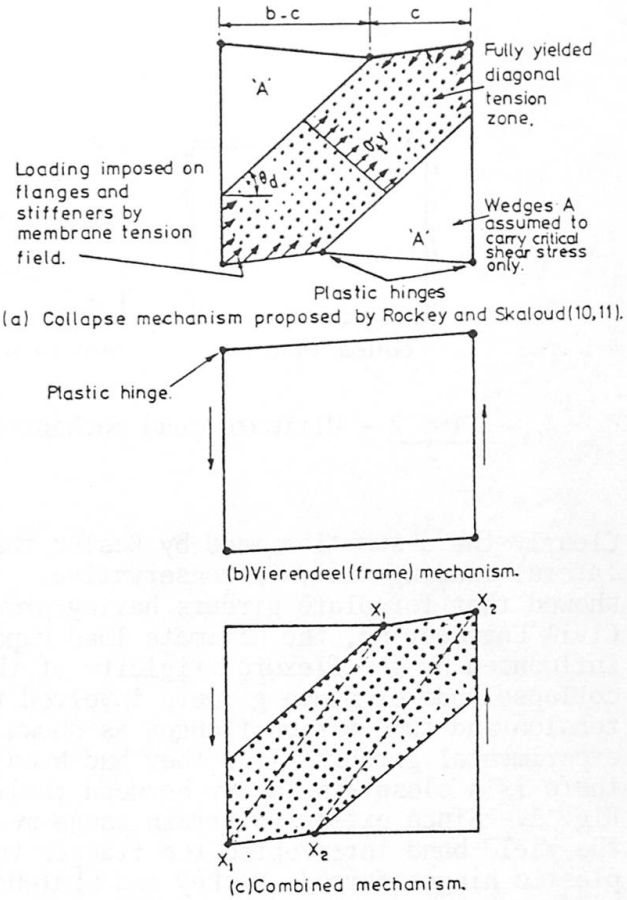


FIG. 3 - Mechanisms involved in collapse of shear panel.

In 1974, the present authors [1,2,3] presented their new collapse mechanism in which a collapse mode similar to that shown in Figs. 3(c) and 7 was considered. It was postulated that in the case of pure shear, failure would occur when the web yields as a result of the combined effect of the inclined membrane field and the buckling stress of the webplate together with the development of plastic hinges in the flanges, as shown in Fig. 7(a). When determining the buckling stress of the webplate it was assumed that the webplate was simply supported

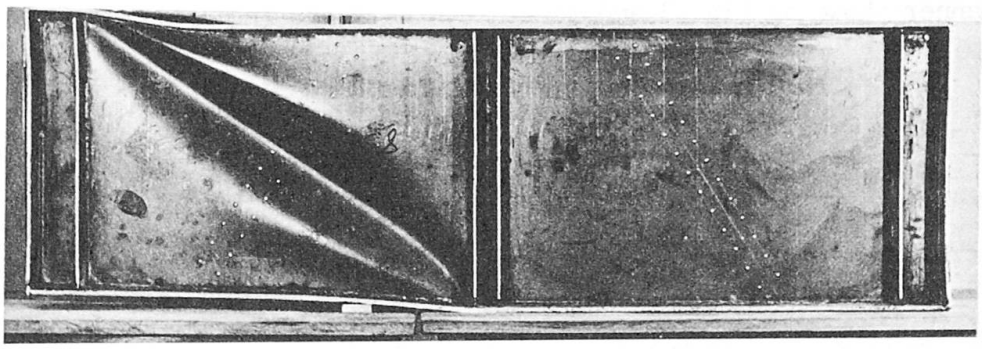

FIG. 4 - View of a failed girder showing failure sway mechanism

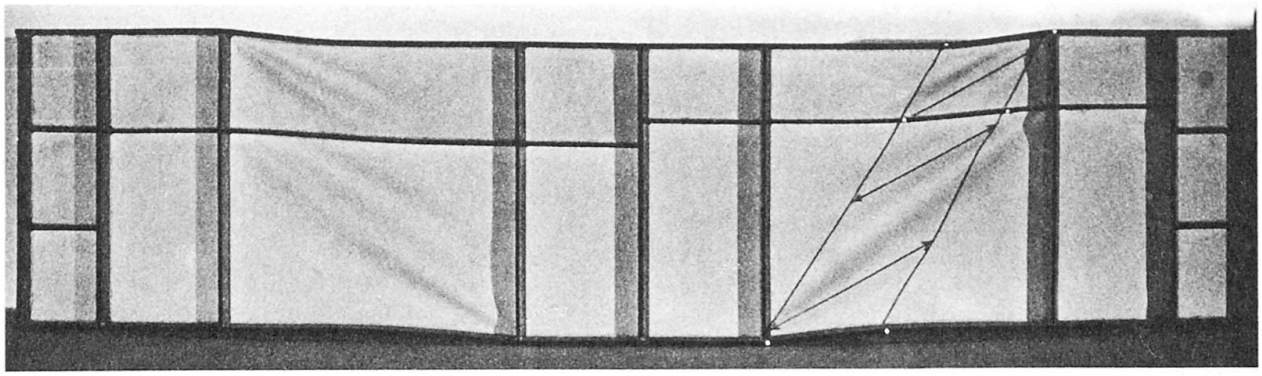

FIG. 5 - Illustration of failure mechanism developed in longitudinally stiffened girders.

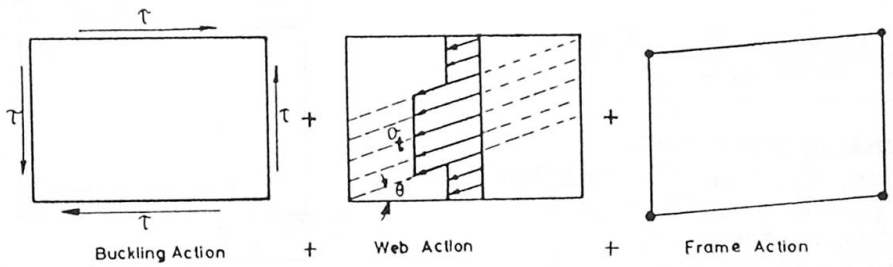


FIG. 6 - Collapse model for a girder panel loaded in shear due to Chern and Ostapenko [14].

along its boundaries. The inclination of the post buckling membrane stress field was taken as a variable in the solution and an optimising process carried out to determine the inclination the maximum load occurs. Since this solution provides the basis of the solutions provided in Section 4, it will be presented in detail.

It was considered that the loading history of a girder could be divided into three phases viz. the two phases shown in Figs. 1(a) and 1(b) and the final collapse stage shown in Fig. 7.

## 2.1 Stage 1 unbuckled behaviour

With a perfectly flat plate there is a uniform shear stress throughout the panel prior to buckling. There will thus be a principal tensile stress of magnitude $\tau$ acting at $45^{o}$ to the flange and a principal compressive stress of the same magnitude acting at $135^{o}$, see Fig. 1(a).

This stress system exists until the shear stress $\tau$ equals the critical shear stress ($\tau_{cr}$). The value of $\tau_{cr}$ for a simply supported rectangular plate can be calculated using equations (1) and (2) :

$$\tau_{cr} = K \left[ \frac{\pi^2 E}{12(1-\mu^2)} \right] \left( \frac{t}{d} \right)^2 \qquad (1)$$

where

$$K = 5.35 + 4 \left( \frac{d}{b} \right)^2 \text{ valid } \frac{b}{d} > 1.0 \qquad K = 5.35 \left( \frac{d}{b} \right)^2 + 4 \text{ valid } \frac{b}{d} < 1.0 \qquad (2)$$

## 2.2 Stage 2 post buckled behaviour

Once the critical shear stress ($\tau_{cr}$) is reached the panel cannot sustain any increase in compressive stress and it buckles. This causes a change in the load carrying system : any additional load has to be supported by a tension membrane field in which the stress has a value of $\sigma_t$, see Fig. 7(a). Under the action of this membrane stress field, the flanges bend inwards and the extent and inclination of the tension membrane stress field which develops is greatly influenced by the rigidity of the flanges.

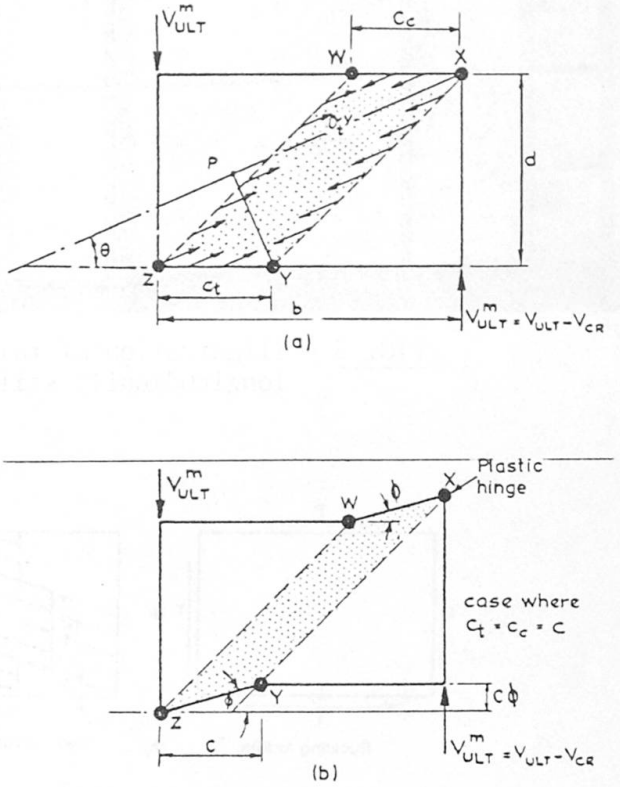


FIG. 7 - Collapse mode for pure shear

## 2.3 Stage 3 determination of the ultimate shear load $V_{ult}$

On further loading the tensile membrane stress, $\sigma_t$, plus the buckling stress, $\tau_{cr}$, produces yielding in the web. The membrane stress which produces yielding is defined as $\sigma_t^y$. Failure occurs when plastic hinges have developed in the flanges and the web has yielded over the zone WXYZ, see Fig. 7. Since there is a uniform shear stress within the webplate, the membrane stress, $\sigma_t^y$, which causes the web to yield is of constant value throughout the yield zone WXYZ. It is a minimum requirement that the region WXYZ must yield before a mechanism can develop. It should be appreciated however that yielding of the webplate is not confined to the zone WXYZ.

The failure load is determined by a consideration of the mechanism developed in Stage 3, see Figs. 3(c) and 7(b). It is convenient to consider the webplate within the region WXYZ to be removed and its action upon the flanges and the adjacent web material replaced by the inclined membrane stresses as shown in Fig. 7(a). Consider a virtual rotation $\phi$ to occur at the flanges to produce the sway mechanism shown in Fig. 7(b). Clearly, the stresses acting on the section ZW do no work and, therefore, only those stresses acting on the inclined right hand web section YX and on the flanges (WX and ZY) will do work. Note, however, that, in the particular case under consideration of a web in shear, if the tension and compression flanges are identical, $c_c$ will be equal to $c_t$ and the work done by the stresses acting on the tension flanges is equal and opposite to that done by the stresses acting on the compression flange. If the flanges have different flexural properties, $c_t$ would not be equal to $c_c$. This is easily allowed for in the authors' general solution; however, for simplicity at this stage, the case of equal flanges has been considered.

The expression for the virtual work done due to a virtual vertical displacement $c\phi$ is given by equation (3) where $V^m_{ult}$ is the post buckling shear load which causes the mechanism to develop.

$$V^m_{ult}\ (c\phi) = 4M_{pf}\phi + \sigma_t^y\ t\ (YP)\ \text{Sin}\ \theta\ (c\phi) \qquad (3)$$

where YP is as defined in Fig. 7(a).

$$V^m_{ult} = \frac{4M_{pf}}{c} + \sigma_t^y \, ct \, \sin^2\theta + \sigma_t^y \, dt \left(\cot\theta - \frac{b}{d}\right) \sin^2\theta$$

The total shear load is equal to the load $V^m_{ult}$ carried by the membrane field and the flanges together with the shear load which causes buckling.

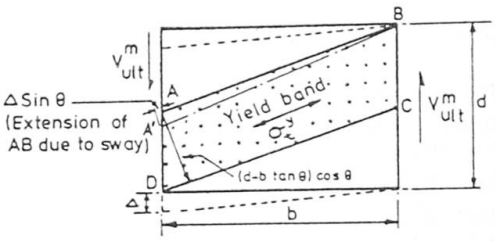


FIG. 8 - Yield band when c = 0 (true Basler solution).

$$\therefore V_{ult} = V^m_{ult} + \tau_{cr} \, dt$$

$$\therefore V_{ult} = \frac{4M_{pf}}{c} + ct \, \sigma_t^y \sin^2\theta + \sigma_t^y \, td \, (\cot\theta - \cot\theta_d) \sin^2\theta + \tau_{cr} \, dt \qquad (4)$$

where $M_{pf}$ is the plastic moment of the flange
$\theta_d$ is the inclination of the panel diagonal
$\theta$ is the inclination of the tension membrane stress field ($\sigma_t^y$).

The value of $\sigma_t^y$ is obtained in equation (5) by applying the Von Mises Hencky yield criterion to the two stress fields which are acting in the webplate i.e. the shear buckling stress and the membrane stress.

$$\sigma_t^y = -\frac{3}{2}\tau_{cr} \sin 2\theta + \sqrt{\sigma^2_{yw} + (\tau_{cr})^2 \left[\frac{9}{4}\sin^2 2\theta - 3\right]} \qquad (5)$$

Since the internal plastic hinge will occur at the point of maximum bending moment where the shear in the flange is zero, it is easy to obtain the position of the internal hinge W by considering the equilibrium of the beam section W - X and taking moments about position X.

$$c(\sigma_t^y \, t) \sin^2\theta \, \frac{c}{2} = 2M_{pf}$$

$$\therefore c = \frac{2}{\sin\theta} \sqrt{\frac{M_{pf}}{\sigma_t^y \, t}} \qquad \text{subject to } c \nmid b \qquad (6)$$

Equation (6) holds for all values of c and for all positive values of $\sigma_t^y$ including the zero value which occurs when the web yields before it buckles. Equation (4) is also valid for all real values of c, i.e. $0 < c < b$. Consider the case where the flanges have no flexural rigidity and, therefore, the yield band is restricted as shown in Fig. 8. Considering the work done by a sway displacement $\Delta$ as shown in Fig. 8 and assuming that the membrane field remains constant within the area ABCD, then the external work, equal to $V^m_{ult}(\Delta)$ must equal the internal work done by the stretching, under constant stress, of strips of the webplate such as AB.

$$V^m_{ult} \times \Delta = (d - b \tan\theta) \cos\theta \, \sigma_t^y \, t \, (\Delta \sin\theta)$$

$$V^m_{ult} = dt \, \sigma_t^y \, (\cot\theta - \cot\theta_d) \sin^2\theta \qquad (7)$$

This is equal to the value given by equation (3) when $M_{pf}$ and, therefore, $c = 0$.

Considering the general case where the flanges can support a membrane stress field, the expression for $V_{ult}$ given in equation (8) is obtained :

$$V_{ult} = \tau_{cr}\, dt + \sigma_t^y\, dt\, \text{Sin}^2\,\theta\, (\text{Cot}\,\theta - \text{Cot}\,\theta_d) + 2\, ct\, \sigma_t^y\, \text{Sin}^2\,\theta \qquad (8)$$

It will be noted that $V_{ult}$ consists of 3 terms, the shear buckling load, the shear load due to the membrane field anchored on to the vertical stiffeners and the shear load due to the membrane field supported by the flanges, see Fig. 9(a). When $M_{pf}$ is zero, then it will be found that the first two terms provide the true Basler solution. For a given girder, the only variable on the right hand side of equation (8) is $\theta$. The only remaining step is now to find that value of $\theta$, ($\theta_m$) which will provide the maximum value of $V_{ult}$. This can be achieved very quickly using a simple desk calculator, especially if one recognises that $\theta_m$ must lie within the region $\theta_d/2 < \theta_m < 45^o$.

Relationships between the non-dimensional parameters c/b, $\theta_m$, $\tau_{ult}/\tau_{yw}$ and the non-dimensional flange-parameter $M_p^*$ (defined in equation (24)) for a given aspect ratio b/d and slenderness ratio d/t, using equation (8), are plotted in Figs. 10 and 11. It will be noted that $\theta$ reaches the values of $45^o$ when c/b = 1.0.

It was established in References [1,2,3] that the Cardiff Solution includes as special cases many of the earlier solutions including the true Basler solution when the flanges have zero flexural rigidity, Calladine's solution for an infinitely thin web and a very thick web, also Wagner's solution and Ostapenko's solution when the flanges are rigid.

The mechanism solution provides an upper bound to the true solution. However, it is also possible to establish an identical equilibrium solution.

The vertical component of the tensile membrane field which acts across section WF in Fig. 9(e) must equal the external shear ($V_{ult} - V_{cr}$).

$$F_s\, \text{Sin}\,\theta = V_{ult} - V_{cr}$$

$$V_{ult} = F_s\, \text{Sin}\,\theta + V_{cr} = \sigma_t^y\, t\, (YP)\, \text{Sin}\,\theta + V_{cr}$$

where YP is as shown in Fig. 7(a).

$$\therefore V_{ult} = V_{cr} + dt\, \sigma_t^y\, \text{Sin}^2\,\theta\, (\text{Cot}\,\theta - \text{Cot}\,\theta_d) + 2\, ct\, \sigma_t^y\, \text{Sin}^2\,\theta$$

This solution is identical to equation (8) which was obtained from the mechanism solution.

It is also possible to obtain a set of forces which will maintain equilibrium in the wedges AWC and YDE, see Fig. 9(a), without violating yield criterion. Consider the yield band to coincide with the internal hinge positions W and Y, then as seen from Fig. 9(b), the flange moment will remain constant at $M_{pf}$ between A and W. If the yield band extends beyond W and Y, then the moment acting between A and W will be reduced as shown in Fig. 9(c). Figure 9(d) shows the distance by which the yield band can extend beyond W and Y before the $M_{pf}$ criterion is violated. The ratio a/c, where a is the width of the tension field acting on the flange, increases with the c/b ratio, as would be expected.

Since the same solution has been obtained using upper and lower bound methods it must be the exact solution for the postulated mode of failure.

Full discussions of the pure shear solution is available in References [1,2,3]

which include its application to the behaviour of webs reinforced by longitudinal stiffeners as well as transverse stiffeners.

## 3. WEBS LOADED IN PURE BENDING

The stress distribution down the depth of a webplate prior to the web buckling is linear, but when the web-plate buckles, part of the web in compression loses its capacity to withstand additional compressive stresses and, as a result, some of the bending moment which should be carried by the compressive area of the webplate is transferred to the flanges. This has a two-fold effect, there is a shift of the neutral axis away from the compression flange with an accompanying increase in the longitudinal strains developed in the compression flange. Figure 12 shows the strains which are developed in a longitudinally reinforced webplate when it was loaded in pure bending [22]. Failure occurs when the compression flange either buckles inwards as shown in Fig. 13, or laterally. In the present study, it will be assumed that the flanges are adequately restrained against lateral buckling. There is evidence [22] to show that the half wave-length of the inward buckle of the compression flange is related to the half wavelength of the compression buckle formed in the webplate. The inward buckling of the compression flange will occur where the bending stress is greatest and will also be in phase with the lateral loading imposed by the membrane

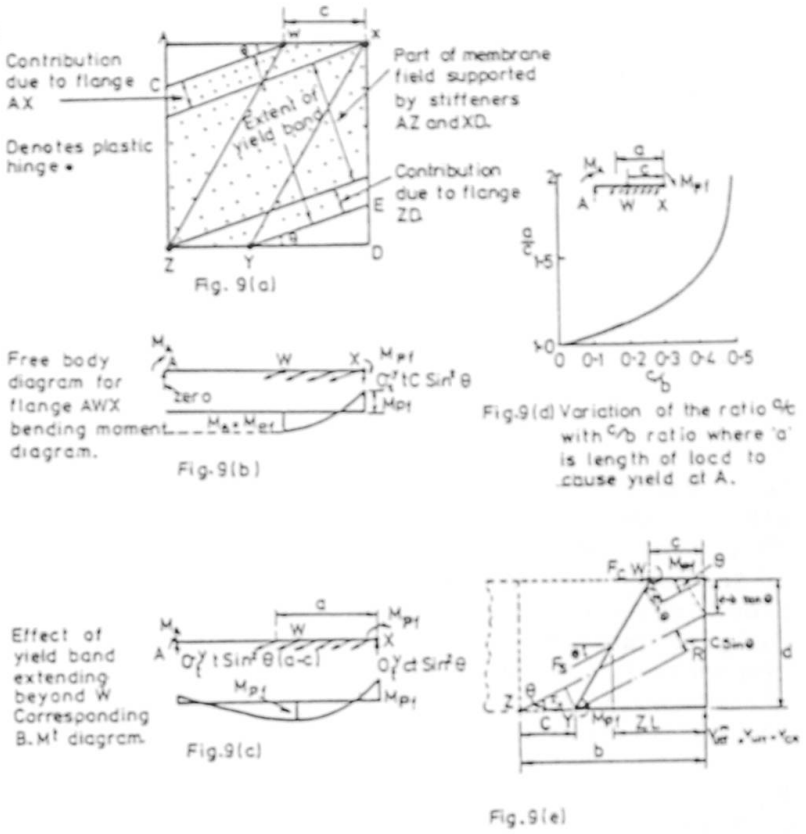


FIG. 9 - Stress conditions in a shear web due to the membrane field.

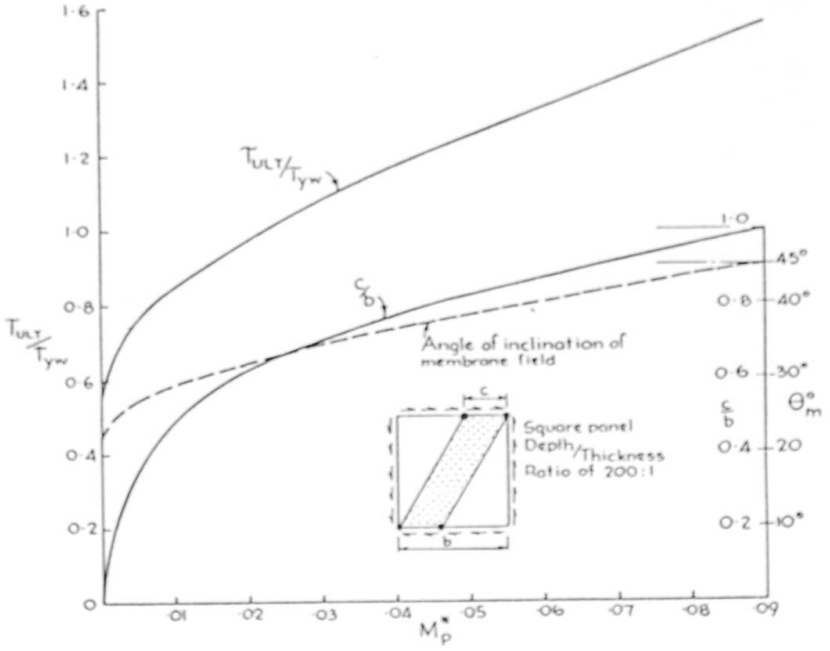


FIG. 10 - Relationship between $\tau_{ult}/\tau_{yw}$, $\theta_m$, c/b and $M_p^*$ for panel of aspect ratio 1 and d/t ratio 200:1. Vertical stiffeners assumed to remain straight.

field developed in the buckled webplate. It is important that the longitudinal stiffeners shall have sufficient flexural rigidity to ensure that they remain straight up to the collapse load of the girder and this has been demonstrated by Massonnet [22,23] and by Owen, Rockey and Skaloud [24] who have recommended the minimum flexural values for longitudinal stiffeners.

In 1960, Basler and Thurlimann [25] reported on a series of tests carried out on welded steel girders. They concluded that, provided lateral buckling of the compression flange was prevented, the ultimate load-carrying capacity of a transversely stiffened plate girder could be predicted by the use of equation (9) :

$$\frac{M_u}{M_y} = 1-0.0005\,\frac{A_w}{A_f}\left(\frac{d}{t}-5.7\sqrt{\frac{E}{\sigma_{yf}}}\right) \quad (9)$$

where $M_y$ is the moment to cause the extreme fibres to yield.

This relationship has been plotted in Fig. 14 from which it will be noted that for values of d/t less than 170:1, the moment to cause collapse is slightly greater than $M_y$, but that for more slender webplates $M_u$ falls below $M_y$. Basler and Thurlimann modified equation (9) to allow for the effect of local or lateral buckling by introducing the critical bending moment $M_{cr}$ as shown in equation (10).

$$\frac{M_u}{M_y} = \frac{M_{cr}}{M_y}\left[1-0.0005\,\frac{A_w}{A_f}\left(\frac{d}{t}-5.7\sqrt{\frac{E}{\sigma_{yf}}}\,\frac{M_y}{M_{cr}}\right)\right] \quad (10)$$

Basler and Thurlimann originally recommended that when $M_u/M_y$ exceeded 1.0, the ultimate load for the girder be

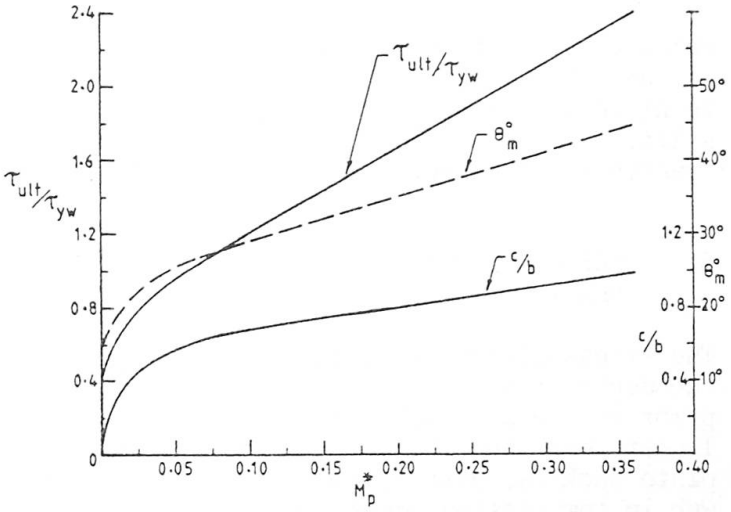


FIG. 11 - Relationship between $\tau_{ult}/\tau_{yw}$, $\theta_m$, c/b and $M_p^*$ for panel with an aspect ratio of 2 and d/t ratio of 200:1.

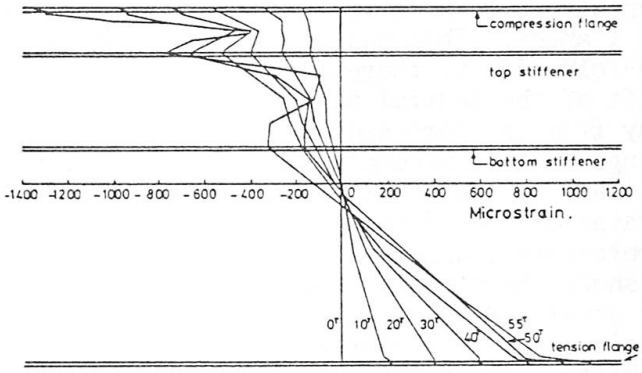


FIG. 12 - Mid plate strains developed in girder TG5-2 when subjected to a bending moment [24].

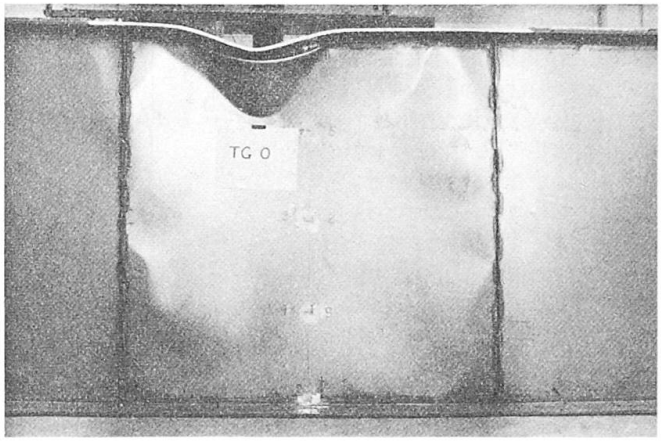


FIG. 13 - Illustration of failure due to inward collapse of compression flange [24].

assumed to be equal to $M_y$. In a subsequent paper Cooper [26] confirmed that equation (10) provides a good prediction of the observed bending strength of full size plate girders, but considered that $M_u$ should be allowed to increase beyond $M_y$ when the d/t ratio is less than 170:1, subject to the limit that $M_u > M_p$, where $M_p$ is the full plastic moment of resistance of the whole girder.

In 1971 Ostapenko, Chern and Parsanejad [28] recommended it was reasonable and accurate to assume that $M_u = M_y$ unless local or lateral buckling of the flange occurred.

In 1971 Maeda [29] reported tests which demonstrated that the formula of Basler and Thurlimann could be used to predict the failure load of conventional plate girders in bending.

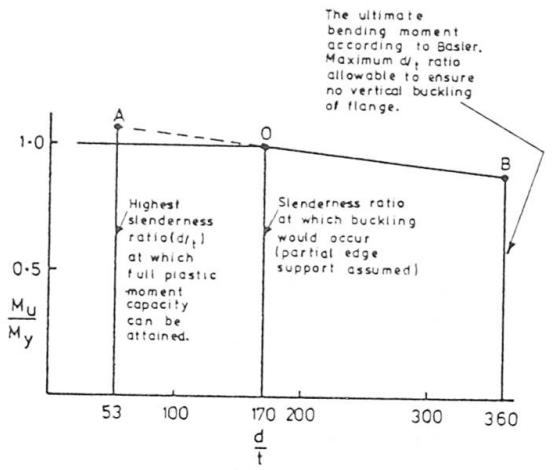


FIG. 14 - Relationship between the ratio $M_u/M_y$ and the d/t ratio as proposed by Basler and Thurlimann [25] ($\sigma_y$ = 30000 psi).

Table 1 compares the ultimate bending stress as provided by equation (10) with the experimental failure loads for a number of plate girders subjected to pure bending. Very satisfactory degree of agreement is obtained, provided $M_u$ is allowed to exceed $M_y$ when the webplates are very thick.

## 4. WEBS SUBJECTED TO SHEAR AND BENDING

The failure mechanism under shear and bending is similar to that for girders loaded in pure shear. Thus, failure occurs when plastic hinges have formed in the flanges, which together with the formation of a yield zone WXYZ in the webplate, form a plastic mechanism, as shown in Fig. 15. It will be noted that, in the case of a girder loaded in shear and bending, $c_c$ is no longer equal to $c_t$.

Four important additional factors must be considered when the effects of bending moment are taken into account.

- The reduction in the buckling stress of the webplate due to the presence of the bending stresses.
- The influence of the bending stresses upon the magnitude of the membrane stresses required to produce yield in the web.
- The influence of load shedding from the web to the flanges as a consequence of buckling.
- The reduction in the plastic moment capacity of the flanges by the axial stresses arising from the bending moment.

These factors will now be considered individually.

- The reduced buckling stress of the webplate due to the presence of the bending stresses may be obtained from the following equation :

$$\left(\frac{\sigma_{mb}}{\sigma_{crb}}\right)^2 + \left(\frac{\tau_m}{\tau_{cr}}\right)^2 = 1 \qquad (11)$$

where

$\sigma_{crb}$ is the critical bending stress when the plate is under the action of a pure bending moment.
$\tau_{cr}$ is the critical shearing stress when the plate is under the action of a pure shearing force.
$\sigma_{mb}$ and $\tau_m$ are the critical bending and shearing stresses respectively for the combined bending and shear loading case.
$\sigma_{mb}$ is the extreme compressive bending stress at the mid panel section.

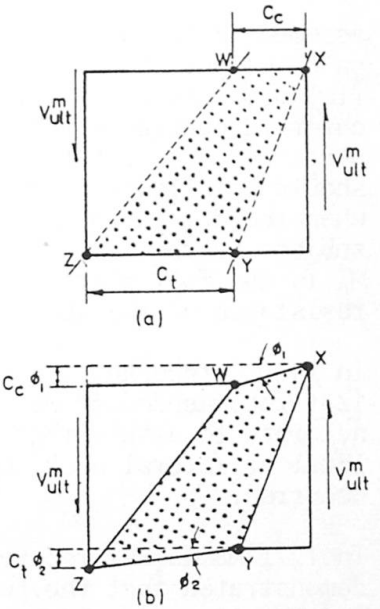


FIG. 15 - Collapse mechanism developed in a panel loaded in shear and bending.

Making the conservative assumption that the web panel is simply supported along each of its four boundaries, the critical pure bending stress is given by equation (12) :

$$\sigma_{crb} = 23.9 \left[ \frac{\pi^2 E}{12(1-\mu^2)} \right] \left( \frac{t}{d} \right)^2 \qquad (12)$$

The value of the membrane stress $\sigma_t^y$ required to produce yielding in the web may be obtained from the Von Mises Hencky yield criterion. For a webplate subjected to both a bending moment and a shearing force, the value of $\sigma_t^y$ at a particular point on the web is given by the following equation :

$$\sigma_t^y = -\frac{1}{2} A + \frac{1}{2} \sqrt{A^2 - 4\left[\sigma_m^2 + 3\tau_m^2 - \sigma_{yw}^2\right]} \qquad (13)$$

where $A = 3\tau_m \, Sin2\theta + \sigma_m Sin^2\theta - 2\sigma_m \, Cos^2\theta$

Since the value of $\sigma_t^y$ varies with the magnitude of the bending stress $\sigma_m$, the value of $\sigma_t^y$ will vary over the area of the webplate and in the establishment of equilibrium equations it is necessary to take into account the variation of $\sigma_t^y$ along the section, see Fig. 16, passing through the hinge positions W and Y. The value of $\sigma_t^y$ is calculated at each of equally spaced stations, Fig. 16(a), across the depth of the section using the appropriate value of $\sigma_m$ for each station. From the membrane stress distribution along the face WY, see Fig. 16(c), the position, direction and magnitude of the total resultant membrane force FW may be obtained, see Fig. 16(b).

The magnitude of the web membrane stress $\sigma_t^y$ will also vary along the length of the junctions between the web and the flange plates. Experience has shown that little loss of accuracy results and a substantial simplification of the solution procedure is achieved if this variation is neglected. Thus a constant value of $\sigma_t^y$ for the flange portion between the hinges has been assumed, evaluated on the basis of the $\sigma_t^y$ value calculated at the mid-point between the hinge positions. Thus, for the compression flange, a constant value $\sigma_{tc}^y$, evaluated mid-way between hinges W and X, has been adopted and for the tension flange a constant value of $\sigma_{tt}^y$, evaluated mid-way between hinges Z and Y.

Because of buckling in the compression region of the webplate, the capacity of the web to carry the applied bending moment is reduced and it is a

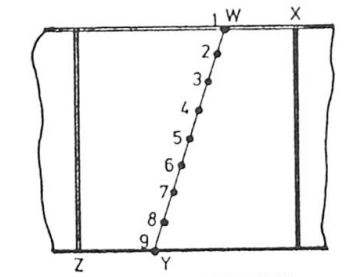


Fig.16a. STATIONS CONSIDERED FOR EVALUATION OF MEMBRANE STRESS FIELD.

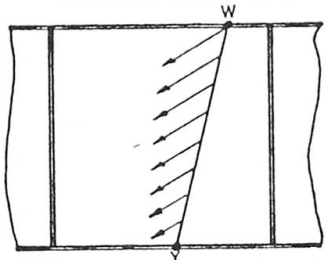


Fig.16c. DISTRIBUTION OF MAGNITUDE OF $\sigma_t^y$ ACROSS FACE W-Y FOR A TYPICAL GIRDER UNDER A HIGH BENDING MOMENT.

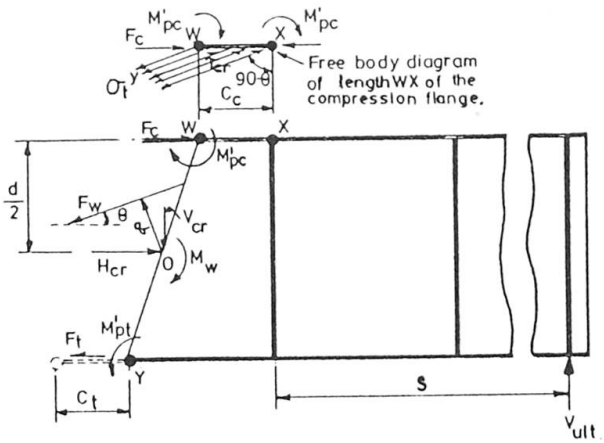


Fig.16b. FREE BODY DIAGRAM OF PORTION OF GIRDER TO THE RIGHT OF CUTTING PLANE W-Y OF A PANEL LOADED IN SHEAR AND BENDING.

simple matter to allow for this reduction in the moment capacity. Since the variation in the value of $\sigma_t^y$ is very small in the compression zone, as shown in Fig. 16(c), the effect of load shedding can be safely neglected.

- The reduced plastic moments of the compression and tension flanges due to the presence of axial forces may be evaluated from the following

$$M'_{pc} = M_{pc}\left[1 - \left(\frac{\sigma_{cf}}{\sigma_{yf}}\right)^2\right] \quad \text{for the compression flange} \qquad (14a)$$

and

$$M'_{pt} = M_{pt}\left[1 - \left(\frac{\sigma_{tf}}{\sigma_{yf}}\right)^2\right] \quad \text{for the tension flange} \qquad (14b)$$

where $\sigma_{yf}$ is the flange yield stress and $\sigma_{cf}$ and $\sigma_{tf}$ are the average stresses in the compression and tension flanges respectively.

The adoption of an average flange stress in the calculation of the reduced flange plastic moment follows from the calculation of an average membrane traction force, as discussed earlier, and leads to a simplified solution procedure. The assumption is justified since, unless the value of $\sigma_m$ is large, the variation in $\sigma_t^y$ will be small and, moreover, when the bending stresses are large the distance between hinges in the compression flange becomes small, so that the variation in the bending stresses, and therefore $\sigma_t^y$, between the two hinges is small. With respect to the tension flange, when the bending stresses are high the value of the membrane stresses acting on the tension flange will be small and therefore the use of an average value for $\sigma_t^y$ is again justified.

## 4.1 Free body diagrams and equilibrium equations

In order to establish the equilibrium equations, a section will be taken between

hinges W and Y. A free body diagram of the portion of the girder to the right of this cutting plane is shown in Fig. 16(b) and all the internal and external forces are shown in the diagram.

Before the reduced flange plastic moments can be calculated from equations 14(a) and 14(b), the average stresses $\sigma_{cf}$ and $\sigma_{tf}$ must be evaluated from a consideration of the equilibrium of the individual flanges.

From the equilibrium of the free body diagram of the portion of the compression flange between hinges W and X shown in Fig. 16(b) :

$$c_c = \frac{2}{\text{Sin } \theta} \sqrt{\frac{M^1_{pc}}{\sigma^y_{tc}\ t}} \tag{15}$$

This equation defines the position of the hinge in the compression flange. It should be noted that the equation is only valid for values of $c_c$ greater than 0 and less than b. In the case of an infinitely weak flange, $M^1_{pc} = 0$, so that the hinge forms at the end of the flange, i.e. $c_c = 0$, and the flange equilibrium equation becomes irrelevant.

Also, the average axial stress in the compression flange may be obtained as :

$$\sigma_{cf} = \frac{F_c - (\sigma^y_{tc} \text{ Sin } \theta \text{ Cos } \theta + \tau_{crm})\ c_c\ t/2}{A_{cf}} \tag{16}$$

where $A_{cf}$ is the cross-sectional area of the compression flange.

Similar for the tension flange :

$$c_t = \frac{2}{\text{Sin } \theta} \sqrt{\frac{M^1_{pt}}{\sigma^y_{tt}\ t}} \tag{17}$$

and

$$\sigma_{tf} = \frac{F_t + (\sigma^y_{tt} \text{ Sin } \theta \text{ Cos } \theta + \tau_{crm})\ c_t\ t/2}{A_{tf}} \tag{18}$$

## 4.2 Overall equilibrium equations

Considering the equilibrium of the portion of the girder to the right of the cutting plane under the action of the forces shown in Fig. 16(b), yields the following equations :

- Resolving vertically $V_{ult} = F_w \text{ Sin } \theta + V_{cr}$ (19)
- Resolving horizontally $F_c - F_t = F_w \text{ Cos } \theta - H_{cr}$ (20)
- Moments about O

$$(F_c + F_t) = \frac{2}{d}\left[ V_{ult}\left[ S + \frac{(b+c_c - c_t)}{2} \right] + M^1_{pt} - M^1_{pc} + F_w q - M_w \right] \tag{21}$$

From these the following expressions are obtained for the flange forces :

$$F_c = \frac{V_{ult}}{d}\left[ \frac{\text{Cot } \theta}{2} d + ZL + \frac{(c_c - c_t)}{2} \right] + \frac{1}{d}\left[ M^1_{pt} + M^1_{pc} + F_w q - M_w \right]$$

$$- \frac{V_{cr}}{2} \text{Cot } \theta - \frac{\tau_{crm}}{2} t\ (b - c_c - c_t) \tag{22}$$

and

$$F_t = \frac{V_{ult}}{d}\left[-\frac{\text{Cot }\Theta}{2}\,d + ZL + \frac{(c_c - c_t)}{2}\right] + \frac{1}{d}\left[M^1_{pt} + M^1_{pc} + F_w q - M_w\right] + \frac{V_{cr}}{2}\,\text{Cot }\Theta + \frac{\tau_{crm}}{2}\,t\,(b - c_c - c_t) \qquad (23)$$

## 4.3 Reduction in shear capacity due to yielding

In some cases, such when the applied bending moment is high and the webplate is thick, it is possible that local yielding will occur before the webplate buckles. No additional post-buckling membrane forces can be developed where yield occurs and the $\sigma_t^y$ values calculated from equation (13) become zero at these positions. This is most likely to occur at hinge position Z where the imposed tensile bending stresses are greatest. An increase in the applied bending moment leads to a growth in the yield zone towards hinge Y. Once this yielding has started to occur and the web membrane forces have become zero, the web no longer exerts the type of traction on the tension flange that has been assumed in the failure mechanism and failure may occur by some other mode. Therefore, in the proposed method, the web is only allowed to carry that amount of bending moment that is sufficient to produce yield, without the addition of membrane forces, at the most susceptible position, i.e. at hinge Z. Any additional bending moment is assumed to be shed from the webplate to the flanges.

## 4.4 Solution procedure

The equations established so far have contained terms involving $\Theta$, the inclination of the membrane field. The inclination at the failure load can be found by assuming successive values of $\Theta$ until the maximum load carrying capacity of the girder ($V_{ult}$) has been determined. Also, for each assumed value of $\Theta$, a closed form solution of the equations (15) to (23), would be extremely difficult. Consequently, an iterative technique has been adopted. In the first cycle of this iteration method, it is assumed that the average flange stresses are zero, and subsequent cycles are then carried out in which more accurate values of the flange stresses are employed. The value of $V_{ult}$ obtained in each cycle is compared to the value obtained from the previous cycle and the process repeated until a satisfactory degree of convergence has been achieved. The rate of convergence in all cases has been found to be extremely rapid.

It is possible to carry out the above solution procedure by "hand", particularly if sufficient experience has been gained so that reasonably accurate values may be chosen as starting points for the two iteration procedures. However, in general, a computer-aided solution would be desirable and full details of a computer programme suitable for a computer with a small storage is given in Ref. [30]. However, recourse to even this simple computer solution is not necessary since, as a result of an extensive parametric study [31], the authors have been able to develop a simple design procedure, details of which are given in the following section.

# 5. DESIGN PROCEDURE

The authors' studies [32] have established that the shear/moment interaction diagram will be of the form shown in Fig. 17. Point S on the interaction diagram gives the shear capacity of the girder i.e. when the influence of any applied bending moments are negligible. Point C corresponds to the situation where the mode of failure of the girder changes from the shear mode to a bending failure mode. Point D corresponds to the maximum bending capacity of conventional plate girders which fail by inward collapse of the compression

flange.

In Section 2 it was shown that the shear capacity of a plate girder is given by equation (8). This equation can now be recast into the following form using $V_s$ to denote the value of the ultimate load in pure shear :

$$\frac{V_s}{V_{yw}} = \frac{\tau_{cr}}{\tau_{yw}} + \sqrt{3}\,\mathrm{Sin}^2\,\theta\left(\mathrm{Cot}\theta - \frac{b}{d}\right)\frac{\sigma_t^{\,y}}{\sigma_{yw}} + 4\sqrt{3}\,\mathrm{Sin}\theta\sqrt{\frac{\sigma_t^{\,y}}{\sigma_{yw}}}\sqrt{M_p^*} \qquad (24)$$

where $M_p^* = \dfrac{M_{pf}}{d^2 t\,\sigma_{yw}}$

When $\tau_{cr}/\tau_{yw} > 0.8$ it is recommended that $\tau_{cr}/\tau_{yw}$ is replaced by the reduced value of $\tau_{cre}/\tau_{yw}$ given by equation (25) :

$$\frac{\tau_{cre}}{\tau_{yw}} = 1 - 0.68\left[\sqrt{\frac{\tau_{yw}}{\tau_{cr}}} - \frac{1}{\sqrt{3}}\right]^2 \qquad (25)$$

$$\text{valid } \frac{1}{\sqrt{3}} < \frac{\tau_{yw}}{\tau_{cr}} < 1.118$$

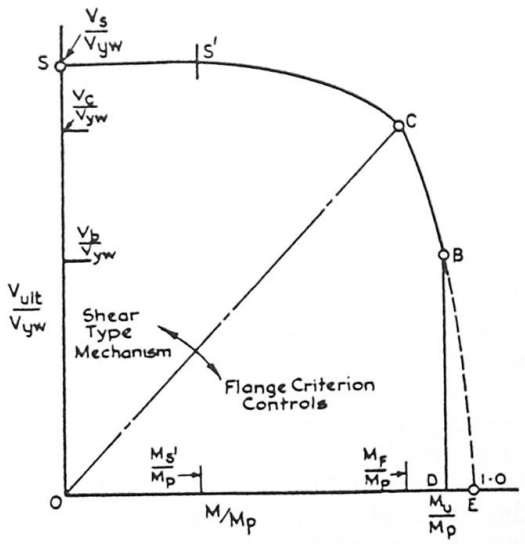


FIG. 17 - Construction of authors' interaction diagram.

In addition to the shear load $V_s/V_{yw}$ given by equation (24), if the flanges of the plate girder are deep, e.g. when wine-glass or tubular flanges are used it will be necessary to allow for the additional shear force $V_f$, carried by both flanges, which is given by equation (26) :

$$V_f = \left(\tau_{cr} + \frac{1}{2}\,\sigma_t^{\,y}\,\mathrm{Sin}2\theta\right) 2a\,t \qquad (26)$$

where a is the distance from the centre of area of the flange to the web/flange junction.

The parametric study conducted by the authors has shown that for girders representative of normal construction, the value of $\theta$ which produces the maximum value of the ratio $V_s/V_{yw}$ is very close to $2/3\,\theta_d$, where $\theta_d$ is the inclination of the panel diagonal to the flange. The assumption of $\theta = 2/3\,\theta_d$ will result in the correct solution or in a slight underestimation of the collapse load.

Assuming that the inclination of the tension membrane field is given by $2/3\,\theta_d$ it is possible to recast equation (24) into the following form :

$$\frac{V_s}{V_{yw}} = A + B\sqrt{M_p^*} + C\,\frac{2a}{d} \qquad (27)$$

where $A = \sqrt{3}\,\mathrm{Sin}^2\theta\left(\mathrm{Cot}\theta - \dfrac{b}{d}\right)\dfrac{\sigma_t^{\,y}}{\sigma_{yw}} + \dfrac{\tau_{cr}}{\tau_{yw}}$

$$B = 4\sqrt{3}\,\mathrm{Sin}\theta\sqrt{\frac{\sigma_t^{\,y}}{\sigma_{yw}}} \qquad C = \left[\frac{\tau_{cr}}{\tau_{yw}} + \frac{\sqrt{3}}{2}\,\mathrm{Sin}2\theta\left(\frac{\sigma_t^{\,y}}{\sigma_{yw}}\right)\right]$$

Values of these coefficients have been calculated and are given in Tables 2 to 4. With the aid of these tables the calculation of $V_s/V_{yw}$ is a simple process.

For practical plate girders, as will be demonstrated later, the use of the above coefficients will provide a safe estimate of the true value of $V_s$. If, however, very strong flanges are used then an improved solution could be obtained by the direct use of equation (24), varying the value of $\theta$ to obtain the maximum value of $V_s$.

The parametric study has also established that the value of the load ratio $V_c/V_{yw}$, corresponding to position C on the interaction diagram, is given by equation (28) :

$$\frac{V_c}{V_{yw}} = \frac{\tau_{cr}}{\tau_{yw}} + \left(\frac{\sigma_t^y}{\sigma_{yw}} \operatorname{Sin} \frac{4\theta d}{3}\right)\left[0.554 + \frac{36.8\, M_{pf}}{M_F}\right]\left[2 - \left(\frac{b}{d}\right)^{\frac{1}{8}}\right] \qquad (28)$$

where $M_{pf}$ = plastic moment of resistance of the flange
$= \frac{1}{4}\sigma_{yf}\, b_f\, t_f^2$ for a single flange plate.
$M_F$ = plastic moment of resistance of the flanges acting alone
$= \sigma_{yf} A_f (d + t_f)$ for single flange plates.

Equation (28) is subject to the limit that $V_c/V_{yw}$ cannot be greater than $V_s/V_{yw}$. If $V_c/V_{yw}$ from equation (28) is greater than $V_s/V_{yw}$, then $V_c$ is taken as equal to $V_s$.

Equation (28) can be recast into the following form :

$$\frac{V_c}{V_{yw}} = \frac{\tau_{cr}}{\tau_{yw}} + D\left[0.554 + \frac{36.8\, M_{pf}}{M_F}\right] \qquad (29)$$

where $D = \left(\frac{\sigma_t^y}{\sigma_{yw}} \operatorname{Sin} \frac{4\theta d}{3}\right)\left[2 - \left(\frac{b}{d}\right)^{\frac{1}{8}}\right]$

Values of coefficient D are given in Table 5.

The authors' study has also established that the interaction diagram S and C is as follows. The shear at $S^1 = V_s b$, where b is the length of the web panel. The bending moment at $S^1$ is subject to the control that its value must not exceed $0.5\, M_F$. A parabola with its origin at $S^1$ is fitted between $S^1$ and C.

Point B corresponds to the situation where the flange fails by inward collapse. The value at which this occurs is given by equation (9).

A study of interaction diagrams has shown that the curve CBE is quite flat and therefore can be safely represented by a simple parabola. Hence the shear load $V_B$ at B acting with $M_u$ is given by equation (30) :

$$\frac{V_B}{V_C} = \sqrt{\frac{M_p - M_u}{M_{pw}}} \qquad (30)$$

where $M_{pw}$ = plastic moment of resistance of web alone.

Thus points S, $S^1$, C, B and D can be calculated very quickly with the aid of Tables 2 to 5 and the relevant equations.

The authors' design method can also be applied to webplates reinforced by both longitudinal and transverse stiffeners (3,30). When calculating the values of

$V_s$ and $V_c$ for a girder with a longitudinally reinforced webplate the value of $\tau_{cr}$ which is employed is the buckling stress of the weakest sub-panel. Using this buckling stress the overall panel is then treated as if it were a transversely reinforced webplate.

## 6. RESULTS

The authors have applied this design process to a large number of test girders. Eighty-eight girders, tested by various investigators have been considered and the result of this study has given a mean value of the ratio of the predicted failure load to the experimental load $V_{pred}/V_{exp}$ of 0.997 with a standard deviation of 0.064. The distribution of the values of $V_{pred}/V_{exp}$ is presented in Fig. 18 which clearly demonstrates the ability of the design method to predict the ultimate load capacity of girders reinforced by both transverse and longitudinal stiffeners accurately.

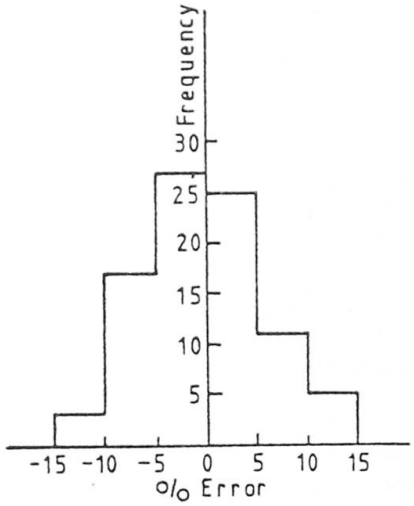


FIG. 18 - Distribution of errors in prediction of failure load for transversely and longitudinally stiffened girders under shear and bending.

TABLE 1

GIRDERS SUBJECTED TO PURE BENDING

| REF | 4 | 31 | 31 | 31 | 31 | 31 | 22 | 32 | 32 | 25 | 22 | 33 | 33 | 33 | 33 |
|---|---|---|---|---|---|---|---|---|---|---|---|---|---|---|---|
| GIRDER | G4T2 | LB1 | LB2 | LB3 | LB4 | LB5 | TTGO | D | 3 | LB6 | TG41 | BL1 | BL2 | BL3 | BL4 |
| d/t | 388 | 444 | 447 | 447 | 447 | 447 | 751 | 299 | 300 | 407 | 751 | 141 | 188 | 234 | 281 |
| $M_u/M_{exp}$ | 0.97 | 1.00 | 1.01 | 1.00 | 0.98 | 0.98 | 0.99 | 1.00 | 0.98 | 1.04 | 1.04 | 1.01 | 0.93 | 0.92 | 0.89 |

REFERENCES

1. ROCKEY, K.C., PORTER, D.M. & EVANS, H.R., "Ultimate load capacity of the webs of thin walled members", Proc. Conf. on Cold Formed Steel Structures, Missouri, St. Louis, 1973, p. 169-200.
2. PORTER, D.M., ROCKEY, K.C. & EVANS, H.R., "The collapse behaviour of plate girders loaded in shear", The Structural Engineer, Vol. 53, Aug. 1975, No. 8, p. 313-325.
3. ROCKEY, K.C., EVANS, H.R. & PORTER, D.M., "The ultimate shear load behaviour of longitudinally reinforced plate girders", TRRL Symposium, U.K., Dec. 1974, p. 162-174.
4. BASLER, K., YEN, B.T., MUELLER, J.A. & THURLIMANN, B., "Web buckling tests on welded plate girders", Weld. Res. Coun. Bull. No. 64, Sept. 1960.
5. BASLER, K., "Strength of plate girders under combined shear and bending", Proc. A.S.C.E. 87 (ST7), 1961, p. 151-180.
6. WAGNER, H., "Ebene Blechwandtrager mit sehr dunnen Stegblechen", Z. Flugtech Motor Luftsch, Vol. 20, 1929, p. 200.
7. WAGNER, H., "Flat sheet metal girders with very thin webs", Part I, II and III, N.A.C.A., TM 604, 605, 606, 1931.
8. KUHN, P. & PETERSON, J.P., "Strength analysis of stiffened beam webs", NACA TN 1364, 1947.
9. KUHN, P., PETERSON, J.P. & LEVIN, C.R., "A summary of diagonal tension parts I and II", NACA T N's 2661 and 2662, 1962.

| $\frac{\tau_{cr}}{\tau_{yw}}$ / $\alpha=\frac{b}{d}$ | 0.8 | 1.0 | 1.2 | 1.4 | 1.6 | 1.8 | 2.0 | 2.2 | 2.4 | 2.6 |
|---|---|---|---|---|---|---|---|---|---|---|
| 0.05 | 0.402 | 0.355 | 0.318 | 0.288 | 0.263 | 0.243 | 0.227 | 0.212 | 0.200 | 0.190 |
| 0.10 | 0.437 | 0.393 | 0.358 | 0.329 | 0.306 | 0.288 | 0.272 | 0.258 | 0.246 | 0.236 |
| 0.15 | 0.471 | 0.430 | 0.397 | 0.371 | 0.349 | 0.331 | 0.316 | 0.303 | 0.292 | 0.283 |
| 0.20 | 0.505 | 0.467 | 0.436 | 0.412 | 0.391 | 0.375 | 0.360 | 0.349 | 0.338 | 0.329 |
| 0.25 | 0.539 | 0.503 | 0.475 | 0.452 | 0.433 | 0.418 | 0.404 | 0.393 | 0.383 | 0.374 |
| 0.30 | 0.573 | 0.539 | 0.513 | 0.492 | 0.475 | 0.460 | 0.448 | 0.437 | 0.428 | 0.420 |
| 0.35 | 0.606 | 0.575 | 0.551 | 0.532 | 0.516 | 0.502 | 0.491 | 0.481 | 0.472 | 0.465 |
| 0.40 | 0.638 | 0.611 | 0.589 | 0.571 | 0.557 | 0.544 | 0.534 | 0.525 | 0.517 | 0.510 |
| 0.45 | 0.671 | 0.646 | 0.626 | 0.610 | 0.597 | 0.586 | 0.576 | 0.568 | 0.560 | 0.554 |
| 0.50 | 0.703 | 0.680 | 0.663 | 0.648 | 0.637 | 0.627 | 0.618 | 0.610 | 0.604 | 0.598 |
| 0.55 | 0.734 | 0.715 | 0.699 | 0.686 | 0.676 | 0.667 | 0.659 | 0.653 | 0.647 | 0.641 |
| 0.60 | 0.766 | 0.748 | 0.735 | 0.724 | 0.715 | 0.707 | 0.700 | 0.694 | 0.689 | 0.685 |
| 0.65 | 0.797 | 0.782 | 0.770 | 0.761 | 0.753 | 0.747 | 0.741 | 0.736 | 0.731 | 0.727 |
| 0.70 | 0.827 | 0.815 | 0.805 | 0.797 | 0.791 | 0.785 | 0.781 | 0.776 | 0.773 | 0.769 |
| 0.75 | 0.857 | 0.847 | 0.839 | 0.833 | 0.828 | 0.824 | 0.820 | 0.816 | 0.813 | 0.810 |
| 0.80 | 0.887 | 0.879 | 0.873 | 0.868 | 0.864 | 0.861 | 0.858 | 0.855 | 0.853 | 0.851 |
| 0.85 | 0.916 | 0.910 | 0.906 | 0.903 | 0.900 | 0.898 | 0.896 | 0.894 | 0.892 | 0.891 |
| 0.90 | 0.944 | 0.941 | 0.938 | 0.936 | 0.934 | 0.933 | 0.932 | 0.931 | 0.930 | 0.929 |
| 0.95 | 0.972 | 0.971 | 0.970 | 0.969 | 0.968 | 0.967 | 0.967 | 0.966 | 0.966 | 0.966 |

TABLE 2 COEFFICIENT A

| $\frac{\tau_{cr}}{\tau_{yw}}$ / $\alpha=\frac{b}{d}$ | 0.8 | 1 | 1.2 | 1.4 | 1.6 | 1.8 | 2 | 2.2 | 2.4 | 2.6 |
|---|---|---|---|---|---|---|---|---|---|---|
| 0.05 | 3.817 | 3.398 | 3.040 | 2.738 | 2.483 | 2.265 | 2.080 | 1.920 | 1.782 | 1.661 |
| 0.10 | 3.733 | 3.328 | 2.982 | 2.689 | 2.441 | 2.231 | 2.050 | 1.894 | 1.759 | 1.641 |
| 0.15 | 3.646 | 3.254 | 2.921 | 2.638 | 2.398 | 2.193 | 2.017 | 1.866 | 1.734 | 1.619 |
| 0.20 | 3.554 | 3.177 | 2.856 | 2.583 | 2.350 | 2.152 | 1.982 | 1.835 | 1.707 | 1.594 |
| 0.25 | 3.458 | 3.096 | 2.787 | 2.524 | 2.300 | 2.109 | 1.944 | 1.801 | 1.677 | 1.568 |
| 0.30 | 3.358 | 3.010 | 2.714 | 2.461 | 2.246 | 2.062 | 1.903 | 1.765 | 1.644 | 1.538 |
| 0.35 | 3.252 | 2.920 | 2.636 | 2.395 | 2.188 | 2.011 | 1.858 | 1.725 | 1.609 | 1.506 |
| 0.40 | 3.140 | 2.824 | 2.553 | 2.323 | 2.126 | 1.957 | 1.810 | 1.682 | 1.570 | 1.471 |
| 0.45 | 3.022 | 2.721 | 2.465 | 2.246 | 2.059 | 1.897 | 1.757 | 1.635 | 1.528 | 1.433 |
| 0.50 | 2.896 | 2.612 | 2.371 | 2.164 | 1.986 | 1.833 | 1.700 | 1.584 | 1.481 | 1.391 |
| 0.55 | 2.762 | 2.496 | 2.268 | 2.074 | 1.907 | 1.763 | 1.637 | 1.527 | 1.430 | 1.344 |
| 0.60 | 2.618 | 2.370 | 2.158 | 1.977 | 1.821 | 1.686 | 1.568 | 1.465 | 1.373 | 1.292 |
| 0.65 | 2.462 | 2.233 | 2.037 | 1.870 | 1.726 | 1.601 | 1.491 | 1.395 | 1.310 | 1.234 |
| 0.70 | 2.292 | 2.082 | 1.904 | 1.752 | 1.620 | 1.506 | 1.405 | 1.317 | 1.238 | 1.168 |
| 0.75 | 2.105 | 1.916 | 1.756 | 1.619 | 1.500 | 1.397 | 1.307 | 1.227 | 1.156 | 1.092 |
| 0.80 | 1.893 | 1.727 | 1.586 | 1.467 | 1.363 | 1.273 | 1.193 | 1.123 | 1.060 | 1.003 |
| 0.85 | 1.650 | 1.508 | 1.389 | 1.288 | 1.200 | 1.124 | 1.056 | 0.997 | 0.943 | 0.895 |
| 0.90 | 1.355 | 1.242 | 1.147 | 1.067 | 0.998 | 0.937 | 0.884 | 0.837 | 0.795 | 0.756 |
| 0.95 | 0.964 | 0.886 | 0.821 | 0.766 | 0.720 | 0.679 | 0.643 | 0.612 | 0.583 | 0.558 |

TABLE 3 COEFFICIENT B

| $\frac{\tau_{cr}}{\tau_{yw}}$ / $\alpha=\frac{b}{d}$ | 0.8 | 1 | 1.2 | 1.4 | 1.6 | 1.8 | 2 | 2.2 | 2.4 | 2.6 |
|---|---|---|---|---|---|---|---|---|---|---|
| 0.05 | 0.823 | 0.771 | 0.718 | 0.667 | 0.619 | 0.577 | 0.539 | 0.505 | 0.475 | 0.449 |
| 0.10 | 0.839 | 0.792 | 0.743 | 0.695 | 0.651 | 0.611 | 0.575 | 0.543 | 0.514 | 0.489 |
| 0.15 | 0.855 | 0.812 | 0.766 | 0.722 | 0.681 | 0.644 | 0.610 | 0.580 | 0.553 | 0.529 |
| 0.20 | 0.870 | 0.831 | 0.789 | 0.748 | 0.710 | 0.675 | 0.644 | 0.616 | 0.590 | 0.567 |
| 0.25 | 0.884 | 0.849 | 0.811 | 0.774 | 0.739 | 0.706 | 0.677 | 0.651 | 0.627 | 0.605 |
| 0.30 | 0.898 | 0.866 | 0.832 | 0.798 | 0.766 | 0.736 | 0.709 | 0.684 | 0.662 | 0.642 |
| 0.35 | 0.911 | 0.883 | 0.852 | 0.822 | 0.792 | 0.765 | 0.740 | 0.717 | 0.697 | 0.678 |
| 0.40 | 0.923 | 0.898 | 0.871 | 0.844 | 0.818 | 0.793 | 0.770 | 0.749 | 0.730 | 0.713 |
| 0.45 | 0.934 | 0.913 | 0.889 | 0.865 | 0.842 | 0.820 | 0.799 | 0.780 | 0.763 | 0.747 |
| 0.50 | 0.945 | 0.927 | 0.906 | 0.885 | 0.864 | 0.845 | 0.827 | 0.810 | 0.794 | 0.779 |
| 0.55 | 0.955 | 0.939 | 0.922 | 0.904 | 0.886 | 0.869 | 0.853 | 0.838 | 0.824 | 0.811 |
| 0.60 | 0.964 | 0.951 | 0.936 | 0.921 | 0.906 | 0.892 | 0.878 | 0.865 | 0.853 | 0.841 |
| 0.65 | 0.972 | 0.962 | 0.950 | 0.938 | 0.925 | 0.913 | 0.901 | 0.890 | 0.880 | 0.870 |
| 0.70 | 0.979 | 0.971 | 0.962 | 0.952 | 0.942 | 0.933 | 0.923 | 0.914 | 0.905 | 0.897 |
| 0.75 | 0.985 | 0.979 | 0.973 | 0.965 | 0.958 | 0.950 | 0.943 | 0.936 | 0.929 | 0.922 |
| 0.80 | 0.990 | 0.986 | 0.982 | 0.977 | 0.972 | 0.966 | 0.961 | 0.956 | 0.950 | 0.945 |
| 0.85 | 0.994 | 0.992 | 0.989 | 0.986 | 0.983 | 0.980 | 0.976 | 0.973 | 0.969 | 0.966 |
| 0.90 | 0.997 | 0.996 | 0.995 | 0.994 | 0.992 | 0.990 | 0.988 | 0.986 | 0.985 | 0.983 |
| 0.95 | 0.999 | 0.999 | 0.999 | 0.998 | 0.998 | 0.997 | 0.997 | 0.996 | 0.996 | 0.995 |

TABLE 4 COEFFICIENT C

| $\frac{\tau_{cr}}{\tau_{yw}}$ / $\alpha=\frac{b}{d}$ | 0.8 | 1.0 | 1.2 | 1.4 | 1.6 | 1.8 | 2.0 | 2.2 | 2.4 | 2.6 |
|---|---|---|---|---|---|---|---|---|---|---|
| 0.05 | .917 | .833 | .753 | .681 | .618 | .562 | .514 | .471 | .434 | .402 |
| 0.10 | .878 | .799 | .725 | .657 | .597 | .545 | .499 | .459 | .423 | .393 |
| 0.15 | .836 | .765 | .695 | .633 | .576 | .527 | .483 | .445 | .411 | .382 |
| 0.20 | .795 | .729 | .665 | .606 | .553 | .507 | .467 | .431 | .398 | .371 |
| 0.25 | .753 | .692 | .633 | .579 | .530 | .487 | .448 | .415 | .385 | .358 |
| 0.30 | .709 | .654 | .601 | .551 | .506 | .465 | .430 | .398 | .370 | .345 |
| 0.35 | .665 | .616 | .567 | .521 | .480 | .444 | .410 | .380 | .355 | .330 |
| 0.40 | .620 | .575 | .531 | .491 | .453 | .419 | .389 | .362 | .337 | .315 |
| 0.45 | .575 | .535 | .495 | .459 | .425 | .394 | .366 | .342 | .319 | .299 |
| 0.50 | .528 | .493 | .459 | .425 | .395 | .368 | .343 | .321 | .300 | .282 |
| 0.55 | .480 | .449 | .419 | .393 | .365 | .341 | .319 | .298 | .280 | .263 |
| 0.60 | .432 | .405 | .380 | .356 | .333 | .312 | .292 | .274 | .258 | .244 |
| 0.65 | .381 | .360 | .338 | .318 | .299 | .281 | .264 | .248 | .234 | .222 |
| 0.70 | .330 | .313 | .296 | .278 | .263 | .248 | .234 | .222 | .210 | .199 |
| 0.75 | .278 | .264 | .252 | .238 | .225 | .214 | .203 | .193 | .182 | .173 |
| 0.80 | .225 | .215 | .206 | .195 | .186 | .178 | .169 | .161 | .154 | .147 |
| 0.85 | .171 | .164 | .157 | .150 | .144 | .139 | .133 | .127 | .121 | .117 |
| 0.90 | .116 | .111 | .107 | .104 | .099 | .096 | .092 | .087 | .084 | .083 |
| 0.95 | .059 | .057 | .055 | .053 | .052 | .051 | .050 | .049 | .046 | .045 |

TABLE 5 COEFFICIENT D

10. ROCKEY, K.C. & SKALOUD, M., "Influence of flange stiffeners upon the load carrying capacity of webs in shear", Proc. 8th Cong. IABSE, New York, 1968, pp. 429-439.
11. ROCKEY, K.C. & SKALOUD, M., "The ultimate load behaviour of plate girders loaded in shear", The Structural Engineer, Vol. 50, No. 1, Jan. 1972, pp. 29-48.
12. FUJII, T., "On an improved theory for Dr. Basler's theory", Proc. 8th Cong. IABSE, New York, Sept. 1968, pp. 477-487.
13. FUJII, T., FUKUMOTO, Y., NISHINO, F. & OKUMURA. T., "Research work on ultimate strength of plate girders and Japanese provisions on plate girder design", Proc. IABSE Colloquium London 1971, pp. 21-48.
14. CHERN, C. & OSTAPENKO, A., "Ultimate strength of plate girders under shear", Fritz Eng. Lab. Report No. 328.7, Lehigh University, Aug. 1969.
15. KOMATSU, S., "Ultimate strength of stiffened plate girders subjected to shear", Proc. IABSE Colloquium, London, 1971, pp. 49-65.
16. Proc. IABSE Colloquium, Design of plate and box girders for ultimate strength, London 1971, (Ed. Massonnet, Rockey and Beedle).
17. OSTAPENKO, A. & CHERN, C., "Ultimate strength of longitudinally stiffened plate girders under combined loads", Proc. IABSE Colloquium London, 1971.
18. ROCKEY, K.C., "An ultimate load method for the design of plate girders", Proc. IABSE Colloquium London, 1971, p. 253-268.
19. CALLADINE, C.R., "A plastic theory for collapse of plate girders under combined shearing force and bending moment", The Structural Engineer, Vol. 51, April 1973, pp. 147-154.
20. LEGGETT, D.M.A. & HOPKINS, H.G., "The effect of flange stiffness on the stresses in a plate web spar under shear", HMSO, R & M No. 2434.
21. BERGMAN, S.G.A., "Behaviour of buckled rectangular plates under the action of shearing forces", Stockholm, 1948.
22. OWEN, D.R.J., ROCKEY, K.C. & SKALOUD, M., "Ultimate load behaviour of longitudinally reinforced webplates subjected to pure bending", IABSE, Vol. 30, 1970, p. 113-148.
23. BASLER, K. & THURLIMANN, B., "Strength of plate girders in bending", Fritz Eng. Lab. Report 251-19, Lehigh University, Nov. 1960.
24. COOPER, P.B., "The ultimate bending moment for plate girders", Proc. IABSE Colloquium, London 1971, p. 291-297.
25. COOPER, P.B., "Bending and shear strength of longitudinally stiffened plate girders", Fritz. Eng. Lab. Report No. 304.6, Lehigh Univ., 1965.
26. OSTAPENKO, A., CHERN, C. & PARSANEJAD, S., "Ultimate strength design of plate girders", Proc. Conference 'Developments in bridge design and construction', Cardiff 1971, Crosby Lockwood & Son, Ltd., p. 505-518.
27. MAEDA, Y., "Ultimate static strength and fatigue behaviour of longitudinally stiffened plate girders in bending", Proc. IABSE Colloquium London 1971, p. 269-282.
28. EVANS, H.R., ROCKEY, K.C. & PORTER, D.M., "A computer programme for determining the ultimate load capacity of a plate girder loaded in shear and bending", Univ. College, Cardiff Report, 1976.
29. EVANS, H.R., PORTER, D.M. & ROCKEY, K.C., "A parametric study of the collapse behaviour of plate girders", Univ. College, Cardiff Report, 1976.
30. ROCKEY, K.C., EVANS, H.R. & PORTER, D.M., "A design method for predicting the collapse behaviour of plate girders", Univ. College, Cardiff Report, 1977.
31. D'APICE, M.A., FIELDING, D.J. & COOPER, P.B., "Static tests on longitudinally stiffened webplates", Welding Res. Council Bull., No. 117, October 1966.
32. LONGBOTTOM, E. & HEYMAN, J., "Experimental verification of the strengths of plate girders design in accordance with the revised British Standard 153 : Tests on full size and on model plate girders", I.C.E., 1956.
33. MAEDA, Y., "Additional study of static strength of hybrid plate girders in bending", IABSE Colloquium, London 1971, p. 409-414.